haematologica
Journal of the Ferrata Storti Foundation

A transgenic mouse model of Down syndrome acute lymphoblastic leukemia identifies targetable vulnerabilities

by Jacob J. Junco, Max Rochette, Michelle Alozie, Raushan Rashid, Maci Terrell, Barry Zorman, Pavel Sumazin, Lauren Rowland, Gino Dettorre, Reid T. Powell, Clifford C. Stephan, Peter J. Davies, Margarita Martinez-Moczygemba, Jun J. Yang, and Karen R. Rabin

Received: November 27, 2023.
Accepted: July 16, 2024.

Citation: Jacob J. Junco, Max Rochette, Michelle Alozie, Raushan Rashid, Maci Terrell, Barry Zorman, Pavel Sumazin, Lauren Rowland, Gino Dettorre, Reid T. Powell, Clifford C. Stephan, Peter J. Davies, Margarita Martinez-Moczygemba, Jun J. Yang, and Karen R. Rabin. A transgenic mouse model of Down syndrome acute lymphoblastic leukemia identifies targetable vulnerabilities. Haematologica. 2024 July 25. doi: 10.3324/haematol.2023.284761 [Epub ahead of print]

A transgenic mouse model of Down syndrome acute lymphoblastic leukemia identifies targetable vulnerabilities

Jacob J. Junco[1], Max Rochette[1], Michelle Alozie[1], Raushan Rashid[1], Maci Terrell[1], Barry Zorman[1], Pavel Sumazin[1], Lauren Rowland[2], Gino Dettorre[2], Reid T. Powell[3,4], Clifford C. Stephan[3,4], Peter J. Davies[3,4], Margarita Martinez-Moczygemba[3,4], Jun J. Yang[2], and Karen R. Rabin[1]

[1]Texas Children's Cancer Center, Department of Pediatrics, Baylor College of Medicine, Houston, TX, USA

[2]Department of Pharmacy and Pharmaceutical Sciences, St. Jude Children's Research Hospital, Memphis, TN, USA

[3]Institute of Biosciences and Technology, Texas A&M University, Houston, TX, USA.

[4]Department of Translational Medical Sciences, School of Medicine, Texas A&M University, Houston, TX, USA.

Corresponding Authors:

Karen R. Rabin

1102 Bates Avenue 750.08, Houston, TX 77030

Phone: 832-824-4213

E-mail: krrabin@texaschildrens.org

Jacob J. Junco

1102 Bates Avenue 750.12F, Houston, TX 77030

Phone: 832-824-4235

E-mail: junco@bcm.edu

Acknowledgments

We thank Roger Reeves and Benjamin Devenney (Johns Hopkins University) for guidance with Dp16 mice. We thank Amos Gaikwad and Tatiana Goltsova of the Texas Children's Cancer Center Flow Cytometry Core Laboratory.

Funding

This research was supported by a Scholar Award from the American Society of Hematology (J.J.J.), the Elsa U. Pardee Foundation (J.J.J.), funding from the NIH (P30 CA125123-12 and R01 CA249867, K.R.R.), grant RP170074 from the Cancer Prevention and Research Institute of Texas (CPRIT) (K.R.R.), the Lynch family (K.R.R.), the Dan L. Duncan Comprehensive Cancer Center, and the John S. Dunn Gulf Coast Consortium for Chemical Genomics. This project was supported by the Cytometry and Cell Sorting Core at Baylor College of Medicine with funding from the CPRIT Core Facility Support Award (CPRIT-RP180672), the NIH (CA125123 and RR024574) and the assistance of Joel M. Sederstrom. This project was supported by the Center for Translational Cancer Research at Texas A&M University with funding from CPRIT grants RP200668 and RP190581.

Author Contributions

J.J.J. designed and conducted experiments, analyzed and interpreted data, and wrote the manuscript. M.R., M.A., R.R, M.T., L.R., and G.D. conducted experiments. B.Z. and P.S. analyzed and interpreted data. R.T.P., C.C.S, P.J.D., M.M.M, and J.J.Y. designed experiments and analyzed and interpreted data. K.R.R. designed experiments, analyzed and interpreted data, and wrote the manuscript. All authors reviewed and approved the manuscript.

Disclosure of Conflicts of Interest

The authors have no conflicts of interest to disclose.

Data sharing statement

The corresponding authors are available to share any requested original data and protocols with other investigators. RNA-Seq data were deposited in the European Nucleotide Archive (ENA), with the accession number PRJEB68384.

Children with Down syndrome (DS) have a 20-fold increased risk of B-acute lymphoblastic leukemia (B-ALL) compared to children without DS.[1] The mechanism underlying the increased risk is not well understood. Outcomes in DS-ALL are poorer than in children without DS, with increased risk of relapse and treatment-related mortality,[2] making it imperative to identify new therapeutic targets to improve outcomes. DS-ALL is notable for harboring *CRLF2*/*JAK2* alterations in 50% of cases,[3,4] demonstrating hyperactive RAS signaling in up to 80% of cases,[5] and exhibiting *PAX5* and *KRAS* mutations in 25% and 15% of cases respectively.[6] Experimental systems are needed to better understand the pathogenesis of DS-ALL and test targeted therapies. Here, we report generation of a *de novo* mouse model and cell lines recapitulating key features of DS-ALL, and demonstrate cytotoxicity of agents which may have efficacy in DS-ALL and other leukemias, including the NAMPT inhibitor FK866 as well as agents targeting DNA damage responses, HSP90, autophagy, and JAK signaling.

We created novel mouse models of DS and non-DS ALL by introducing $Kras^{G12D}$ and *Pax5* heterozygosity, both driven by *CD19-Cre*, in the Dp16 mouse model of DS[7] and in littermate control wild-type (WT) mice. $Kras^{G12D}.Pax5^{+/-}$ mice on both Dp16 and WT backgrounds developed highly penetrant B-ALL, with 8/9 Dp16 and 23/23 WT moribund leukemic mice demonstrating expansion of a B progenitor population (typically $B220^{+}CD43^{+}CD24^{+}CD25^{+}$, Figure 1A) in the bone marrow, spleen, and lymph nodes (Figure 1B). Notably, the Dp16 $Kras^{G12D}.Pax5^{+/-}$ B-ALL mice had a significantly shorter latency to disease than WT $Kras^{G12D}.Pax5^{+/-}$ B-ALL mice (80 vs 114 days, $p<0.0001$). Dp16 mice with either $Kras^{G12D}$ or *Pax5* heterozygosity alone also developed leukemias significantly earlier and at greater penetrance than WT mice with these alterations ($p<0.05$), but with a longer latency and less complete penetrance than mice bearing both alterations (Figure 1C). While Dp16 $Pax5^{+/-}$ mice developed B-ALL, Dp16 or WT $Kras^{G12D}$ mice typically developed myeloid or T-cell disease (*Online Supplementary Figures S1A-C*). We confirmed disease

transplantability by injecting splenic blasts from leukemic Dp16 and WT *Kras*^{G12D}*.Pax5*$^{+/-}$ mice into NSG mice. Most primary samples (7/8 WT, 7/8 Dp16) generated leukemia in one or more recipient mice, with marrow and splenic infiltration with blasts of the same B-progenitor immunophenotype as the primary cells. There was no difference in survival in NSG recipient mice of WT vs Dp16 B-ALL blasts (*Online Supplementary Figures S1D-E*). All animal experiments were performed with approval of the Baylor College of Medicine Institutional Animal Care and Use Committee. Next, we generated immortal B-ALL cell lines from 5 Dp16 and 2 WT *Kras*^{G12D}*.Pax5*$^{+/-}$ mice by incubating splenic blasts isolated from secondary NSG mouse xenografts with IL-7-supplemented medium for at least one month. These B-ALL lines displayed a B220^{+}CD43^{+}CD24^{+}CD25^{+} B progenitor immunophenotype, similar to that of primary mouse samples (*Online Supplementary Figure S1F*), and maintained the presence of the Dp16 transgene (data not shown).

We performed whole transcriptome sequencing to characterize NSG-expanded Dp16 and WT *Kras*^{G12D}*.Pax5*$^{+/-}$ B-ALL blasts compared to control early B-lineage (B220+) bone marrow (BM) cells from age-matched healthy Dp16 and WT mice. Gene set enrichment analysis (GSEA) using Hallmark gene sets demonstrated increased expression of oncogenic Myc targets and oxidative phosphorylation associated genes in both B-ALL models (Figure 2A), as well as upregulation of common human B-ALL oncogenes (including *Kras* and *Flt3*) and downregulation of genes frequently inactivated in human B-ALL (including *Ikzf1* and *Pax5*)[6,8] (*Online Supplementary Figure S2A*). The Dp16 *Kras*^{G12D}*.Pax5*$^{+/-}$ B-ALL model also displayed significant upregulation of DNA repair signaling compared to healthy Dp16 control B cells (Figure 2A). We also compared gene expression in Dp16 and WT control B cells. Genes upregulated in human DS vs non-DS lymphoid cells,[9] including *Dyrk1a*, *Runx1*, *Hmgn1*, *Rcan1*, *Ifnar1*, *Ifnar2*, and *Ifngr2*, were among the top upregulated genes in Dp16 vs WT B cells (*Online Supplementary Figure S2B*).

We conducted whole exome sequencing to determine if Dp16 and WT *Kras*^{G12D}*.Pax5*$^{+/-}$ B-ALL have secondary alterations common in human leukemia. We observed 8/8 leukemias arising independently in mice had an additional mutation in *Pax5* and/or *Ikzf1*, and 6/8 had alterations in epigenetic-associated genes, alterations also commonly observed in both DS and non-DS ALL.[6,8] Interestingly, 5/6 mice with additional *Pax5* alterations had a *Tox* mutation, alterations also observed to co-occur in human B-ALL (Figure 2B).[10]

Next, we performed drug screens in the Dp16 and WT *Kras*^{G12D}*.Pax5*$^{+/-}$ B-ALL cell lines and four DS-ALL patient samples to evaluate novel therapeutic agents. We performed a high-throughput screen with the Broad Institute Informer Set in two Dp16 and two WT *Kras*^{G12D}*.Pax5*$^{+/-}$ B-ALL cell lines. Inhibitors of mitosis, DNA damage response, and kinases were effective in all four cell lines. Only the HSP90 inhibitor AT13387 was significantly more effective in the Dp16 vs WT *Kras*^{G12D}*.Pax5*$^{+/-}$ B-ALL cell lines (34.01 vs 47.5 nM, p=0.04, *Online Supplementary Figure S3A*). We also performed cytotoxicity testing using a custom leukemia panel of 35 agents. We found that luminespib, bortezomib, inotuzumab, JQ1, palbociclib, vorinostat, and most kinase inhibitors reduced viability of at least 3/4 B-ALL cell lines and 2/4 DS-ALL patient samples at nanomolar-range concentrations. Many other compounds tested were effective in all mouse B-ALL cell lines, but only in one DS-ALL patient sample, potentially due to heterogeneity of these cases (*Online Supplementary Figure S3B*).

We chose the most effective drugs from the custom leukemia panel and the Broad Institute Informer Set high-throughput screen, and identified from prior work,[11] for testing in PDX-expanded DS and non-DS B-ALL patient samples. All patient samples were collected with informed consent under a protocol approved by the Baylor College of Medicine Institutional Review Board. We selected agents which had demonstrated cytotoxicity in the Dp16 *Kras*^{G12D}*.Pax5*$^{+/-}$ B-ALL cell lines and DS-ALL patient samples, and have shown good

bioavailability and safety profiles in prior mouse xenograft studies and/or potential clinical utility in phase I trials. Most tested agents significantly reduced the viability of both DS-ALL and non-DS ALL patient samples (Figure 3A). There were no significant differences in sensitivity based on DS vs non-DS or *CRLF2*-mutated vs *CRLF2*-wild-type status. DS-ALL and non-DS ALL samples were most sensitive to therapies targeting the DNA damage response (dinaciclib), autophagy (bafilomycin A1), JAK signaling (cucurbitacin I), and glycolysis (FK866). We confirmed the on-target mechanism of FK866 cytotoxicity via inhibition of the glycolytic enzyme NAMPT, by demonstrating that NAD+ supplementation in K187 cells prevented cytotoxicity of FK866 but not doxorubicin (Figure 3B). Finally, we tested two effective agents, FK866 and cucurbitacin I, *in vivo* in mice xenografted with *CRLF2*/*JAK2*-mutated DS-ALL patient samples 839 and K187. Cucurbitacin I modestly reduced peripheral blood (PB) disease burden of 839-xenografted mice and had no effect on PB or BM burden or spleen weights of K187-xenografted mice (*Online Supplementary Figures S3C-E*). FK866 significantly reduced PB burden of both 839 and K187-xenografted mice throughout treatment, and reduced spleen weight and BM burden of K187 mice (Figures 3C-E).

Other mouse models and cell lines recapitulating DS-ALL have been developed, but require viral transduction and/or transplantation into WT mice.[12,13] To generate our novel syngeneic DS-ALL mouse model, we chose the Dp16 mouse model because it contains a large complement of Hsa21 orthologues, including the Down syndrome critical region, and we induced $Kras^{G12D}$, *Pax5* heterozygosity, or both specifically in B cells via CD19-mediated Cre expression. The latency to disease for each genotype ($Kras^{G12D}.Pax5^{+/-}$, $Kras^{G12D}$, and $Pax5^{+/-}$) was significantly shorter for Dp16 than for WT mice, demonstrating the leukemogenic effect of the Dp16 genetic background. Importantly, this DS-ALL mouse model contains a fully native marrow microenvironment and immune system, providing a valuable opportunity to study interactions between native DS BM cell populations and developing B-ALL.

Triplication of specific Hsa21 genes likely directly contributes to the increased risk of DS-ALL, and Hsa21 genes *DYRK1A* and *HMGN1* may be therapeutic targets in DS-ALL.[12,13] We observed *Dyrk1a*, *Hmgn1*, and *Runx1* were significantly upregulated in Dp16 BM B cells compared to WT, supporting utility of our model for studies of novel therapies. We also observed upregulation of *Ifnar1*, *Ifnar2*, and *Ifngr2*, paralleling a key feature of immune dysregulation observed in DS,[14] which may contribute to features associated with DS-ALL.

Despite differences in latency to disease between the Dp16 and WT B-ALL mouse models, the GSEA analyses and mouse cell line drug screening revealed limited biological differences between the blasts in each model. Both the Dp16 and WT B-ALL cells demonstrated upregulation of pathways involving Myc signaling and oxidative phosphorylation, and both mouse and human DS and non-DS B-ALL cells were similarly sensitive to novel therapeutic agents. These results parallel another chemosensitivity study, which showed equal sensitivity of DS and non-DS ALL samples to several chemotherapies.[15] Finally, NSG recipients of established Dp16 and WT *Kras*^{G12D}*.Pax5*$^{+/-}$ leukemic blasts demonstrated the same latency to disease. Overall, our findings suggest the main difference between the Dp16 and WT *Kras*^{G12D}*.Pax5*$^{+/-}$ models is in timing of leukemia initiation, rather than features of the resulting leukemic blasts.

The Dp16 *Kras*^{G12D}*.Pax5*$^{+/-}$ B-ALL mouse model presented here is a powerful tool for studies of DS-ALL. It constitutes a *de novo* ALL in a DS model organism with a native stromal microenvironment and immune system, and demonstrates a transcriptome profile and secondary alterations that recapitulate key features of DS-ALL. Our *in vitro* screen identified several new agents with potential utility in DS and non-DS ALL, and our *in vivo* DS-ALL PDX studies confirmed cytotoxicity of the NAMPT inhibitor FK866.

References

1. Hasle H, Clemmensen IH, Mikkelsen M. Risks of leukaemia and solid tumours in individuals with Down's syndrome. Lancet. 2000;355(9199):165-169.

2. Buitenkamp TD, Izraeli S, Zimmermann M, et al. Acute lymphoblastic leukemia in children with Down syndrome: a retrospective analysis from the Ponte di Legno study group. Blood. 2014;123(1):70-77.

3. Hertzberg L, Vendramini E, Ganmore I, et al. Down syndrome acute lymphoblastic leukemia, a highly heterogeneous disease in which aberrant expression of CRLF2 is associated with mutated JAK2: a report from the International BFM Study Group. Blood. 2010;115(5):1006-1017.

4. Mullighan CG, Collins-Underwood JR, Phillips LA, et al. Rearrangement of CRLF2 in B-progenitor- and Down syndrome-associated acute lymphoblastic leukemia. NatGenet. 2009;41(11):1243-1246.

5. Koschut D, Ray D, Li Z, et al. RAS-protein activation but not mutation status is an outcome predictor and unifying therapeutic target for high-risk acute lymphoblastic leukemia. Oncogene. 2021;40(4):746-762.

6. Li Z, Chang TC, Junco JJ, et al. Genomic landscape of Down syndrome-associated acute lymphoblastic leukemia. Blood. 2023;142(2):172-184.

7. Li Z, Yu T, Morishima M, et al. Duplication of the entire 22.9 Mb human chromosome 21 syntenic region on mouse chromosome 16 causes cardiovascular and gastrointestinal abnormalities. Hum Mol Genet. 2007;16(11):1359-1366.

8. Brady SW, Roberts KG, Gu Z, et al. The genomic landscape of pediatric acute lymphoblastic leukemia. Nat Genet. 2022;54(9):1376-1389.

9. Sullivan KD, Lewis HC, Hill AA, et al. Trisomy 21 consistently activates the interferon response. Elife. 2016;5:e16220.

10. Zaliova M, Stuchly J, Winkowska L, et al. Genomic landscape of pediatric B-other acute lymphoblastic leukemia in a consecutive European cohort. Haematologica. 2019;104(7):1396-1406.

11. Schraw JM, Junco JJ, Brown AL, Scheurer ME, Rabin KR, Lupo PJ. Metabolomic profiling identifies pathways associated with minimal residual disease in childhood acute lymphoblastic leukaemia. EBioMedicine. 2019;48:49-57.

12. Carey-Smith SL, Simad MH, Panchal K, et al. Efficacy of DYRK1A inhibitors in novel models of Down syndrome acute lymphoblastic leukemia. Haematologica. 2024;109(7):2309-2315.

13. Lane AA, Chapuy B, Lin CY, et al. Triplication of a 21q22 region contributes to B cell transformation through HMGN1 overexpression and loss of histone H3 Lys27 trimethylation. Nat Genet. 2014;46(6):618-623.

14. Galbraith MD, Rachubinski AL, Smith KP, et al. Multidimensional definition of the interferonopathy of Down syndrome and its response to JAK inhibition. Sci Adv. 2023;9(26):eadg6218.

15. Zwaan CM, Kaspers GJ, Pieters R, et al. Different drug sensitivity profiles of acute myeloid and lymphoblastic leukemia and normal peripheral blood mononuclear cells in children with and without Down syndrome. Blood. 2002;99(1):245-251.

Figure Legends

Figure 1: *Kras^{G12D}.Pax5$^{+/-}$* mice develop B-acute lymphoblastic leukemia (B-ALL), with a shorter latency in the Dp16 versus WT background. (A) Nearly all moribund *Kras^{G12D}.Pax5$^{+/-}$* mice (23/23 wild-type wild-type (WT), 8/9 Dp16) assayed by flow cytometry demonstrated expansion of a B-ALL, typically B220^{+}CD43^{+}CD24^{+}CD25^{+}, in the blood, bone marrow, and spleen relative to age-matched healthy control Dp16 and WT mice. Representative dot plots from splenic cells are shown. **(B)** Dp16 *Kras^{G12D}.Pax5$^{+/-}$* and WT *Kras^{G12D}.Pax5$^{+/-}$* mice demonstrated enlarged spleens and lymph nodes compared to non-leukemic control Dp16 and WT mice (*p<0.05, **p<0.001, ***p<0.0001, Mann-Whitney U test). **(C)** Dp16 *Kras^{G12D}.Pax5$^{+/-}$* and WT *Kras^{G12D}.Pax5$^{+/-}$* mice developed B-ALL with high penetrance, with a significantly shorter median latency in Dp16 *Kras^{G12D}.Pax5$^{+/-}$* compared to WT *Kras^{G12D}.Pax5$^{+/-}$* mice (80 vs 114 days, p<0.0001, log-rank test). Latency to disease was also shorter in Dp16 *Kras^{G12D}* compared to WT *Kras^{G12D}* mice (p=0.01), and Dp16 *Pax5$^{+/-}$* compared to WT *Pax5$^{+/-}$* mice (p<0.01). Mice were monitored for at least 500 days.

Figure 2. Dp16 and WT *Kras^{G12D}.Pax5$^{+/-}$* B-ALL recapitulate gene expression signatures and co-occurring mutations commonly seen in human B-ALL. **(A)** Gene set enrichment analysis revealed significant upregulation of Myc targets and oxidative phosphorylation in both Nod scid gamma (NSG)-expanded Dp16 *Kras^{G12D}.Pax5$^{+/-}$* and WT *Kras^{G12D}.Pax5$^{+/-}$* B-ALL compared to healthy Dp16 and WT BM B cells. DNA repair genes were also significantly upregulated in Dp16 *Kras^{G12D}.Pax5$^{+/-}$* B-ALL. Approximate Normalized Enrichment Score (NES) and False Discovery Rate (FDR) q-values are indicated by colors and size of circles (legend at right, significant FDR q-value<0.05, n=4 for B-ALL groups, n=5 for healthy control BM B cells). **(B)** Whole exome sequencing revealed both Dp16 *Kras^{G12D}.Pax5$^{+/-}$* and WT *Kras^{G12D}.Pax5$^{+/-}$* B-ALL have mutations in genes and pathways also frequently mutated in human B-ALL, including those involved in B-cell development and epigenetic regulation (n=4, mouse IDs indicated at top

of each column, only non-synonymous mutations with a variant allele frequency ≥20% are shown).

Figure 3. Targeted agents are effective against Down syndrome (DS)-ALL and non-DS ALL patient samples *in vitro*, and FK866 reduces DS-ALL disease burden *in vivo*. (A) DS-ALL and non-DS ALL patient samples were incubated with 12 targeted therapies selected from the two screening studies, and 3 standard chemotherapies (doxorubicin, vincristine, and dexamethasone). Cells were incubated with each drug at 11 doses from ~1 nM to 4 μM for 72 hours, before viability was measured with CellTiter-Glo. Bafilomycin A1, FK866, dinaciclib, and cucurbitacin I were effective in all patient samples at low nanomolar concentrations. Samples with IC_{50} values above 10 μM are not displayed. **(B)** Blasts isolated from a mouse xenografted with DS-ALL patient sample K187 were pretreated with NAD+ (triangles) or vehicle (circles), before 72 hr incubation with up to 250 nM doxorubicin (black) or FK866 (blue). The effect of FK866 was selectively reversed by NAD+ supplementation, indicating FK866 functions by inhibiting NAMPT (*p<0.0001, Student's t-test). **(C)** NSG mice xenografted with DS-ALL patient samples K187 (circles) or 839 (triangles) were treated with vehicle (black) or 20 mg/kg FK866 (blue) via i.p. injection 5 days per week for 4 weeks. FK866 significantly reduced PB disease burden at all tested timepoints during treatment. By 1 week post-treatment, there was no difference in PB blast burden between groups (*p<0.05, **p<0.01, Student's t-test, investigators were blinded to PB sample identity). FK866 also significantly reduced **(D)** spleen weight and **(E)** BM leukemic disease burden after 4 weeks of treatment in K187 mice (n=4, *p<0.05, **p<0.01, Student's t-test).

Figure 1

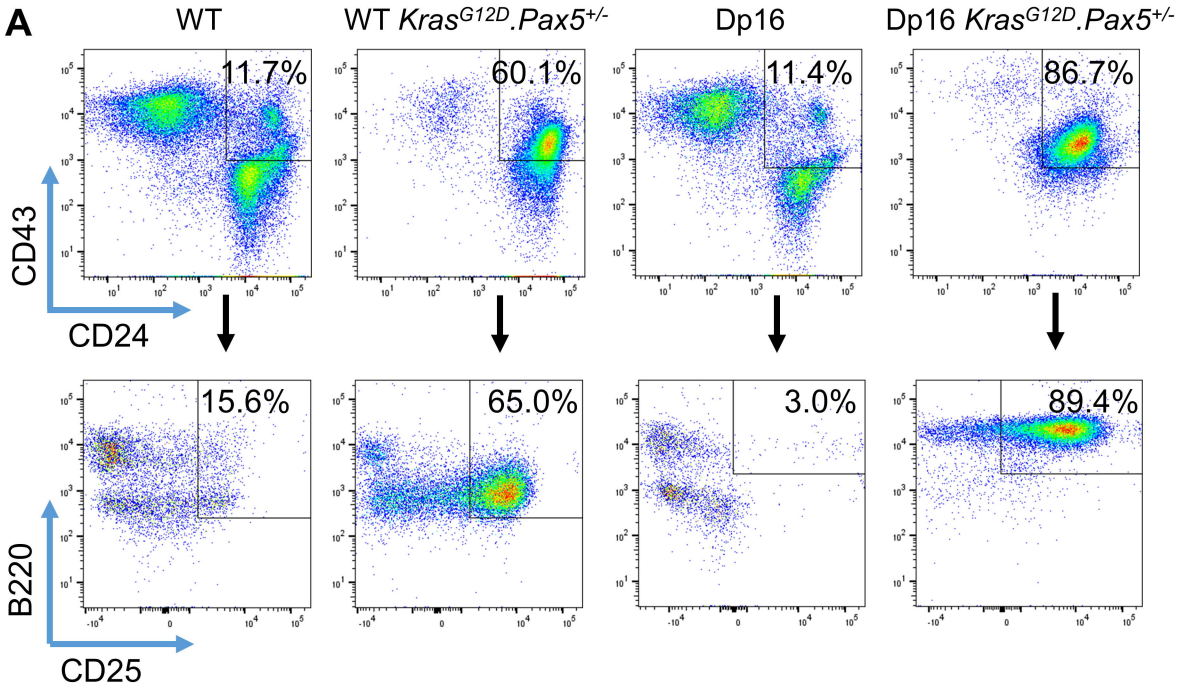
A
WT
WT Kras^G12D.Pax5^+/-
Dp16
Dp16 Kras^G12D.Pax5^+/-
11.7%
60.1%
11.4%
86.7%
CD43
CD24
15.6%
65.0%
3.0%
89.4%
B220
CD25

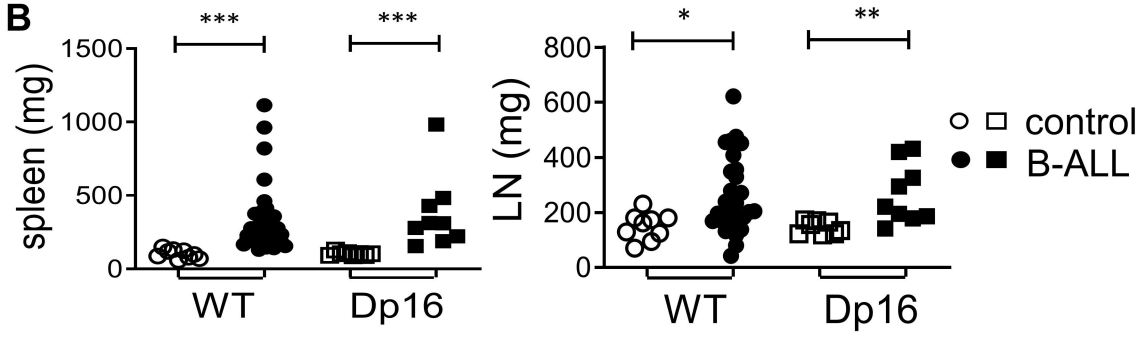
B
***
***
*
**
spleen (mg)
1500
1000
500
0
LN (mg)
800
600
400
200
0
WT
Dp16
WT
Dp16
control
B-ALL

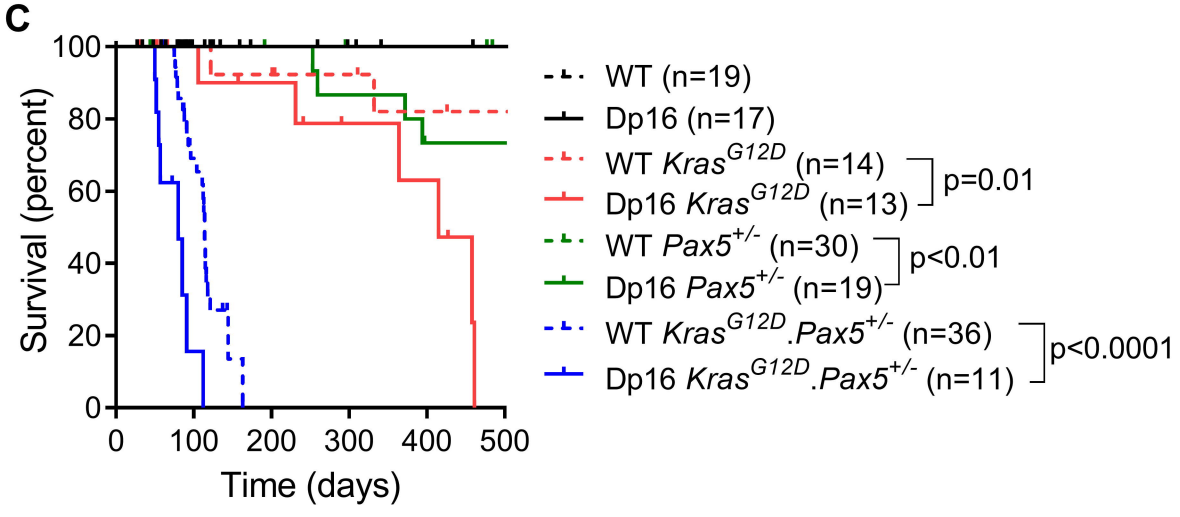
C
Survival (percent)
100
80
60
40
20
0
0
100
200
300
400
500
Time (days)
WT (n=19)
Dp16 (n=17)
WT Kras^G12D (n=14)
Dp16 Kras^G12D (n=13)
p=0.01
WT Pax5^+/- (n=30)
Dp16 Pax5^+/- (n=19)
p<0.01
WT Kras^G12D.Pax5^+/- (n=36)
Dp16 Kras^G12D.Pax5^+/- (n=11)
p<0.0001

Figure 2

A

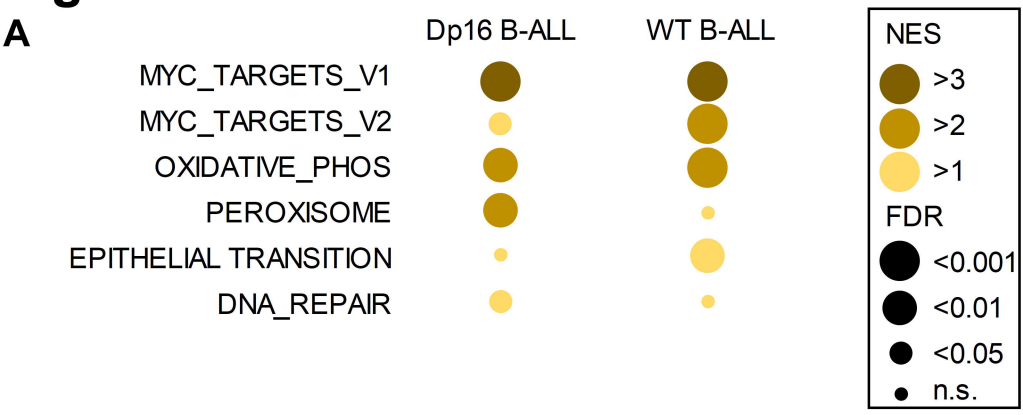

B

Pathway	Gene	Dp16 B-ALL 599	Dp16 B-ALL 631	Dp16 B-ALL 707	Dp16 B-ALL 713	WT B-ALL 625	WT B-ALL 626	WT B-ALL 677	WT B-ALL 683
RAS	*Kras*	G12D	G12D	G12D	G12D	G12D	G12D	G12D	G12D
B-cell pathway/ lymphoid	*Bcl11a*		L147P						
	Ebf1							Q32R	
	Ikzf1				G205Rfs*2	S251_S387del		C332_E333inG	R75L
	Pax5	P80R	S86P	G85R			P316T	V26Gfs*49	R38C
	Tox	E140D	E140D	E140D				E140D	E140D
Epigenetic/ Remodeller	*Arid1a*								W1546R
	Arid5b							N480S	
	Asxl1	A1467T							
	Chd4					L75P			
	Ezh2						E116K		
	Kdm6b	K979Rfs*104							
	Kmt2a			E806D, E821P					E806D, E821P
	Kmt2b								P1120L
	Kmt2d					Q2786R			
JAK-STAT	*Tyk2*	H261R							
Kinase	*Abl1*						S857G		
	Pdgfrb	R703Q							
Transcription	*Elf1*				E103K				
	Gata3	L102Q							
	Zfhx3						L1726S		
Membrane	*Gnas*		Q510R						
	Muc4			start SNV					
DNA repair	*Atm*			R32C, Q1078H, A2119T					R32C, Q1078H, A2119T
Others	*Cux1*			A1423V					
	Serp2				A34T				
	Syne1	V1597L							E1291Q

Missense
Frameshift
Nonsense
In-frame insertion
Start-loss

Figure 3

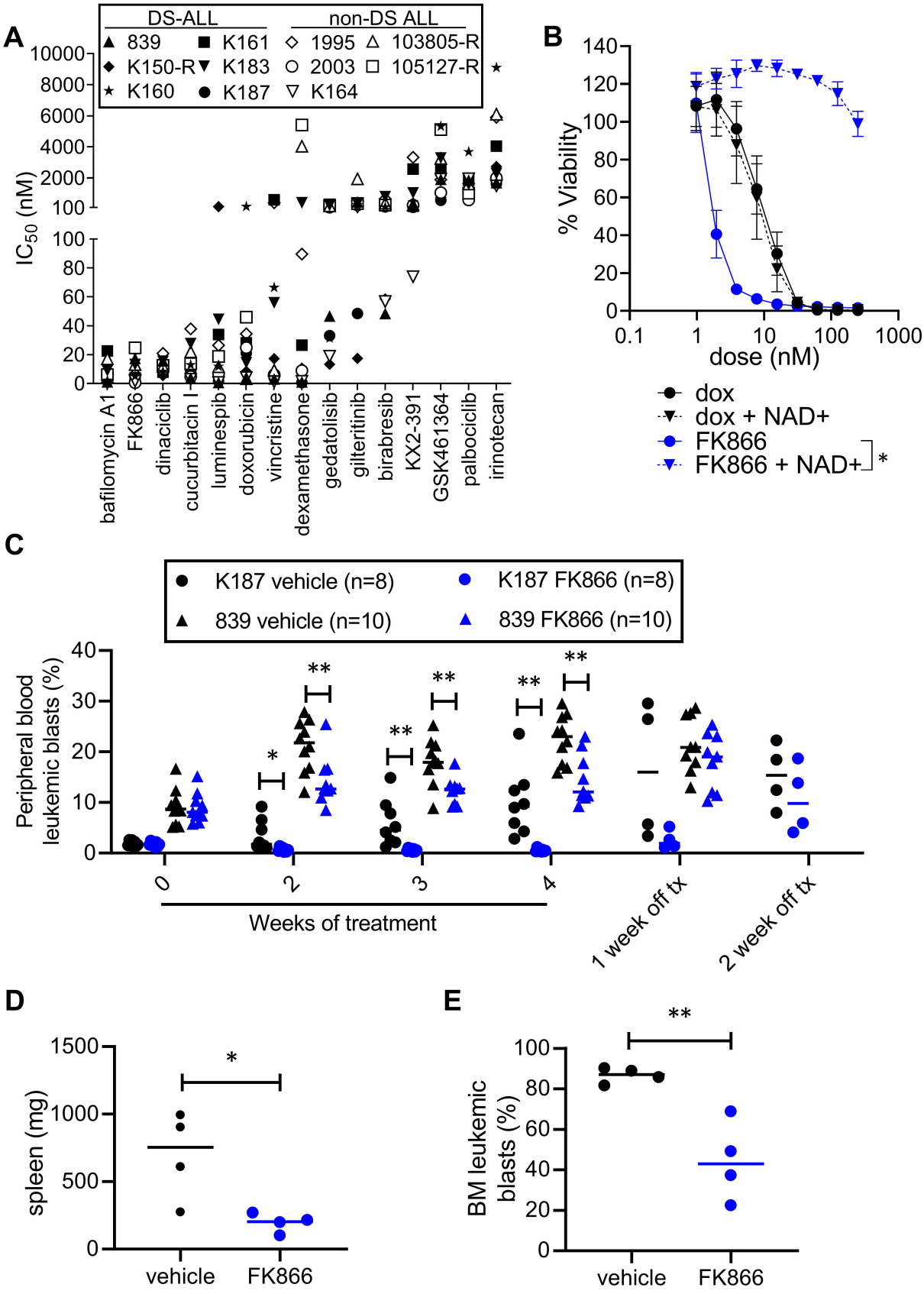
A
DS-ALL
839
K150-R
K160
K161
K183
K187
non-DS ALL
1995
2003
K164
103805-R
105127-R
IC50 (nM)
bafilomycin A1
FK866
dinaciclib
cucurbitacin I
luminespib
doxorubicin
vincristine
dexamethasone
gedatolisib
gilteritinib
birabresib
KX2-391
GSK461364
palbociclib
irinotecan
B
% Viability
dose (nM)
dox
dox + NAD+
FK866
FK866 + NAD+
*
C
K187 vehicle (n=8)
839 vehicle (n=10)
K187 FK866 (n=8)
839 FK866 (n=10)
Peripheral blood leukemic blasts (%)
Weeks of treatment
1 week off tx
2 week off tx
D
spleen (mg)
vehicle
FK866
E
BM leukemic blasts (%)
vehicle
FK866

A transgenic mouse model of Down syndrome acute lymphoblastic leukemia identifies targetable vulnerabilities

Supplementary Figures

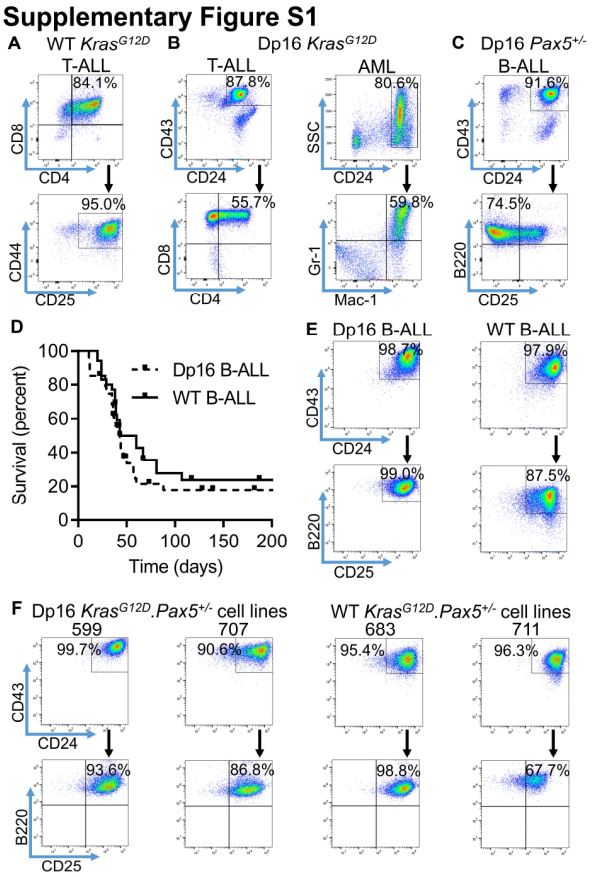

Supplementary Figure S1. Dp16 and WT *Kras^{G12D}* mice develop leukemias of different lineages, and NSG recipients of Dp16 and WT *Kras^{G12D}.Pax5$^{+/-}$* B-ALL cells develop B-ALL with similar latency and the same immunophenotype as the primary sample and generate novel B-ALL cell lines. (A) WT *Kras^{G12D}* mice (n=2) developed disease with an immunophenotype consistent with T-ALL. **(B)** Dp16 *Kras^{G12D}* mice developed disease with an immunophenotype consistent with T-ALL (n=2) or acute myeloid leukemia (n=4). **(C)** Dp16 *Pax5$^{+/-}$* mice (n=4) developed disease with an immunophenotype consistent with B-ALL. For **(A-C)**, representative dot plots from spleen cells are shown. **(D)** NSG recipients of Dp16 or WT B-ALL primary samples both had a median latency to disease of 43 days (p=0.25). **(E)** Spleen cells from leukemic NSG recipients demonstrated a high burden of disease with the same B-ALL immunophenotype (typically B220$^+$CD43$^+$CD24$^+$CD25$^+$) as the primary mouse sample (representative Dp16 and WT samples shown). **(F)** The two Dp16 (599 and 707) and two WT (683 and 711) *Kras^{G12D}.Pax5$^{+/-}$* B-ALL lines used in drug screening experiments displayed a B220$^+$CD43$^+$CD24$^+$CD25$^+$ immunophenotype, similar to the primary mouse leukemia samples. Three additional Dp16 *Kras^{G12D}.Pax5$^{+/-}$* B-ALL lines displayed a similar immunophenotype (data not shown).

Supplementary Figure S2

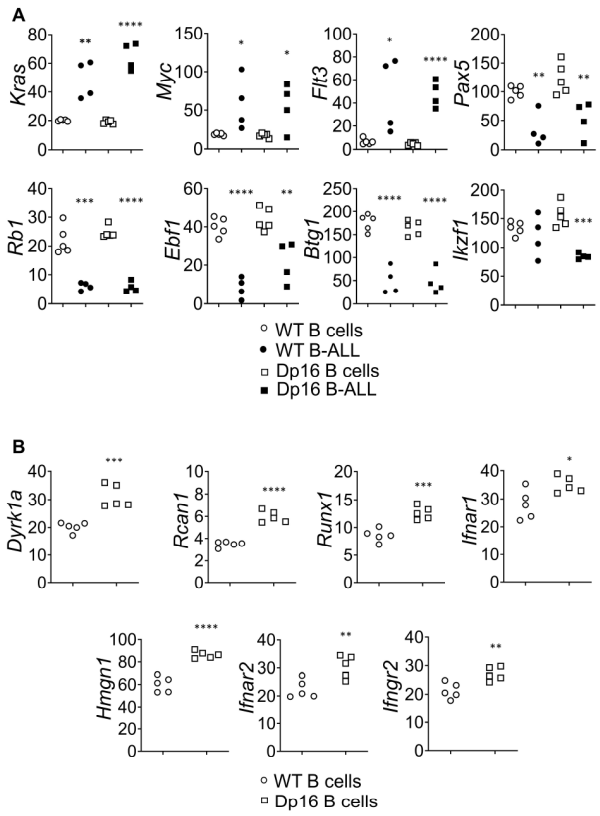

Supplementary Figure S2. Dp16 and WT *Kras^{G12D}.Pax5$^{+/-}$* B-ALL, and Dp16 and WT non-leukemic bone marrow B cells, demonstrate gene expression changes similar to human cells. (A) Expression of genes in signaling pathways frequently activated in B-ALL, including *Kras*, *Myc,* and *Flt3,* were significantly upregulated in both the Dp16 and WT *Kras^{G12D}.Pax5$^{+/-}$* B-ALL models compared to control B cells. The expression of tumor suppressor genes frequently mutated in DS-ALL and non-DS ALL, including *Pax5*, *Ikzf1*, *Rb1*, *Ebf1*, and *Btg1*, were significantly downregulated in the Dp16 *Kras^{G12D}.Pax5$^{+/-}$* B-ALL model compared to control Dp16 B cells. *Pax5*, *Rb1*, *Ebf1*, and *Btg1* were also significantly downregulated in WT *Kras^{G12D}.Pax5$^{+/-}$* B-ALL compared to control WT B cells (*p<0.05, **p<0.01, ***p<0.001, ****p<0.0001 for significance relative to B cell control for each genotype, Student's t-test). **(B)** A number of genes shown to be upregulated in DS lymphoblastoid cells were significantly upregulated in B220+ BM B cells from Dp16 compared to WT healthy non-leukemic mice (*p<0.05, **p<0.01, ***p<0.001, ****p<0.0001 for significance relative to WT BM B cells, Student's t-test). Fragments Per Kilobase of transcript per Million mapped reads (FPKM) values are displayed.

Supplementary Figure S3

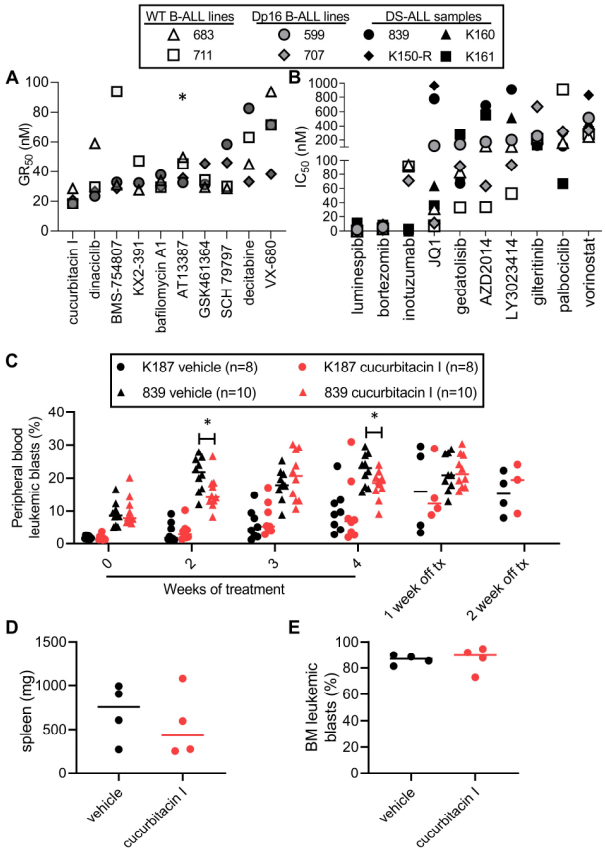

Supplementary Figure S3. Dp16 and WT B-ALL lines and DS-ALL patient samples are sensitive to novel targeted agents, and cucurbitacin I displays limited efficacy *in vivo*. (A) Two Dp16 and two WT *Kras*^{G12D}*.Pax5*$^{+/-}$ B-ALL cell lines were tested in a high-throughput screen using the Broad Institute Informer Set. Cells were incubated with 10 nM, 100 nM, or 1 µM of drug for 72 hours before viable cells were quantified using a flow cytometry-based assay. Of 365 unique small molecules tested, 44 reduced the growth of all four tested B-ALL cell lines. For clarity, the individual GR_{50} values (in nM) for the 10 most effective agents inhibiting the growth of all four cell lines are shown (*$p<0.05$ for the average GR_{50} in Dp16 vs WT). **(B)** Cell lines were incubated with a targeted panel of 35 drugs for 72 hours prior to CellTiter-Glo viability assay. DS-ALL patient samples were incubated in the same panel for 96 hours prior to imaging assays. The 10 compounds displayed were effective at nanomolar-range concentrations in most tested samples. Samples which were insensitive to any particular drug are not displayed. IC_{50} values in nM are indicated. The legend for both **(A)** and **(B)** is indicated above. **(C)** NSG mice xenografted with DS-ALL patient samples K187 (circles) or 839 (triangles) were treated with vehicle (black) or 1 mg/kg cucurbitacin I (red) via i.p. injection 5 days per week for 4 weeks. Cucurbitacin I significantly reduced PB disease burden at weeks 2 and 4 of the treatment phase in mice xenografted with DS-ALL 839, but had no effect in mice with DS-ALL K187 (*$p<0.05$, Student's t-test, investigators were blinded to PB sample identity). Cucurbitacin I had no effect on **(D)** spleen weight or **(E)** BM leukemic disease burden after 4 weeks of treatment in K187 mice (n=4).